Latest Results from the Front End Test Stand High Performance H^- Ion Source at RAL

D. C. Faircloth, S. R. Lawrie, A. P. Letchford, C. Gabor, M. Whitehead, T. Wood and M. Perkins

STFC, Rutherford Appleton Laboratory, Chilton, Didcot, Oxfordshire OX11 0QX, United Kingdom.

Abstract. The aim of the Front End Test Stand (FETS) project is to demonstrate that chopped low energy beams of high quality can be produced. FETS consists of a high power Penning Surface Plasma Ion Source, a 3 solenoid LEBT, a 3 MeV RFQ, a chopper and a comprehensive suite of diagnostics. This paper briefly outlines the status of the project, hardware installation and modifications. Results from experiments running the H^- ion source at 2 ms pulse length are detailed: the discharge current is varied between 20 A and 50 A. The discharge repetition rate is varied between 12.5 and 50 Hz. Hydrogen and Caesium vapour flow rates are varied. The effect of electrode surface temperature and beam current droop are discussed. Peak beam currents of over 60 mA for 2 ms pulse length can be achieved. Normalised r.m.s emittances of 0.3 πmm.mrads at the exit of the LEBT are presented for different source conditions.

Keywords: High performance negative hydrogen ion sources
PACS: 07.77.Ka

INTRODUCTION

The Front End Test Stand (FETS)

FETS is being developed as a generic injector for future high power proton particle accelerators. The aim of the FETS is to demonstrate the production of a 60 mA, 2 ms, 50 pps chopped H^- beam at 3 MeV with sufficient beam quality for future applications. FETS consists of a high power ion source, a 3 solenoid magnetic Low Energy Beam Transport (LEBT), a 324 MHz, 3 MeV, 4-vane Radio Frequency Quadrupole (RFQ), a fast electrostatic chopper and a comprehensive suite of diagnostics.

Present Status

At the time of writing the ion source, LEBT and some of the diagnostics are operational. Figure 1 shows the present status of the FETS beam line. A moveable diagnostics vessel is mounted on the end of the beam line directly after the third LEBT solenoid. The position of four beam current toroids labelled T1 to T4 are shown in figure 1.

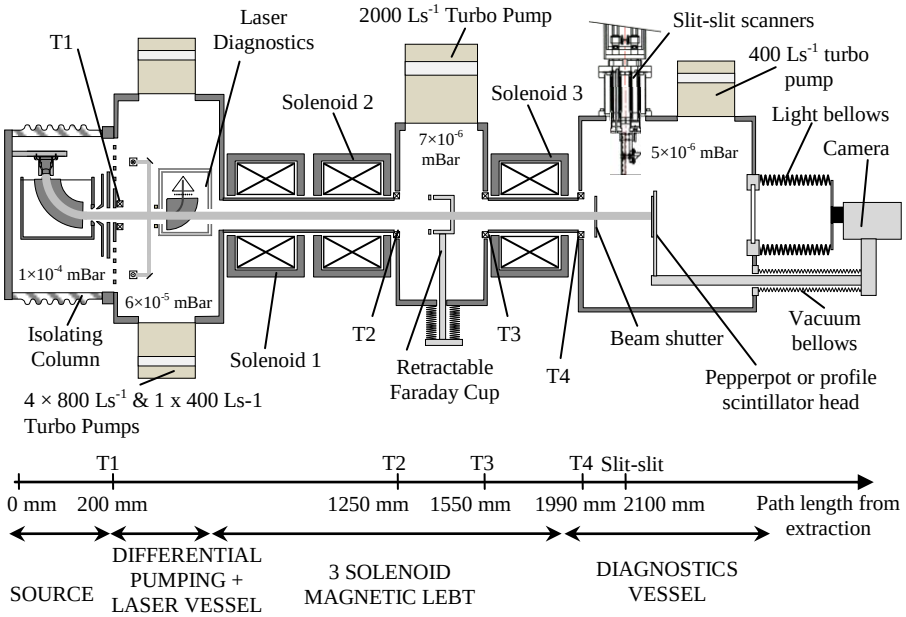

FIGURE 1. Schematic showing the present status of the FETS beam line.

Beam Line Development

RFQ

An RFQ cold model has been manufactured and tested and used to validate an electromagnetic model of the RFQ. Tuners and associated control systems have been built and tested. An integrated CAD/FEA system has been developed to design the RFQ vane modulations. Machining, bonding and vacuum sealing tests have allowed a strategy for manufacturing the RFQ to be developed. A detailed thermal model has validated the cooling scheme. High temperature stability cooling plant has been installed along with the 2 MW klystron RF power supply. The time span for manufacture of the RFQ is now dependent on the uncertain financial climate.

Chopper and MEBT

The design of the chopper is nearly complete, several prototypes of chopper components have been manufactured. Particle tracking in the MEBT has been undertaken and initial quadrupole magnet designs produced.

Laser Beam Diagnostics

A laser on loan from Frankfurt University has been used to progress the development of the laser profile measurement system. There have been significant problems with the acceptance of the electron detection system making it very sensitive to beam fluctuations. A proof of principle experiment has demonstrated photo-detachment, but more development work is required before a working profile measurement system can be achieved.

Ion Source

FETS ion source

The FETS ion source has been described in detail previously [1]. The source is of the Penning type. A schematic of the plasma source and the extraction system is shown in figure 2.

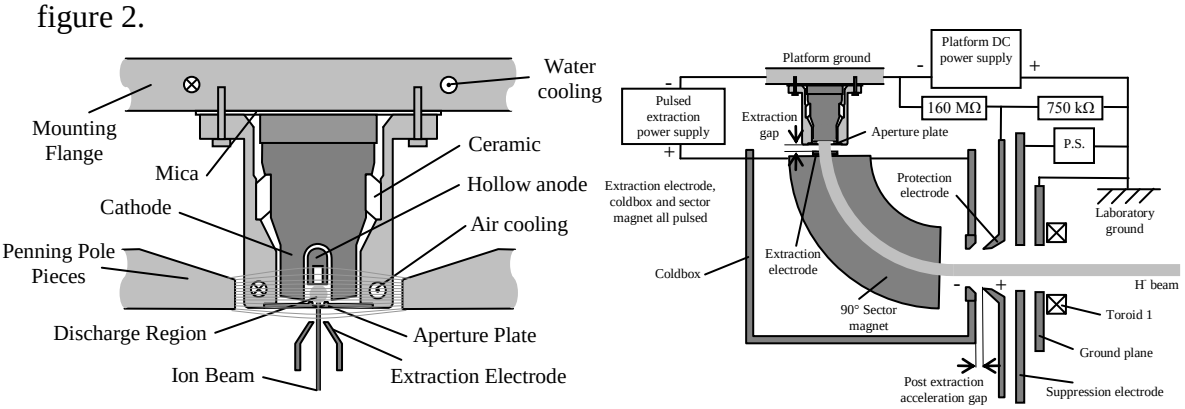

FIGURE 2. A schematic of the FETS ion source and extraction system.

Discharge Power Supply Modifications

The existing source discharge power supply is a pulsed current source capable of delivering up to 90 A, 1 ms long pulses at 50 Hz. The discharge power supply is designed and constructed in house and has successfully driven the plasma on the ISIS ion source for about 10 years. The power output stage consists of 4 IGBTs driven in linear mode to produce a current regulated output. FETS requires beam current pulse lengths of up to 2 ms. To achieve this, a discharge longer than 2 ms must be produced. This provides a settling time for the discharge and power supply so that beam can extracted from a stable plasma. By adding an extra 2 IGBTs to the output stage the power supply can generate current pulses up to 2.2 ms long at 50 Hz. The output current however is limited to about 55 A at this duty cycle.

EXPERIMENTS

Vary Discharge Current

Figure 3 shows the discharge current and voltage oscilloscope traces for different discharge currents for a 2.2 ms long discharge pulse. The pulsed discharge power supply is current regulated so that flat current pulses can be produced. For discharge currents below 30 A the plasma takes up to 300 μs to stabilise which produces a substantial amount of ringing on the front of the discharge pulse due to the lower plasma density.

The discharge voltage slowly drops along the length of the discharge. The discharge voltage increases for lower discharge currents.

For each discharge current, the ion source cooling is modified to keep the electrode temperatures approximately constant and the source is given time to stabilise.

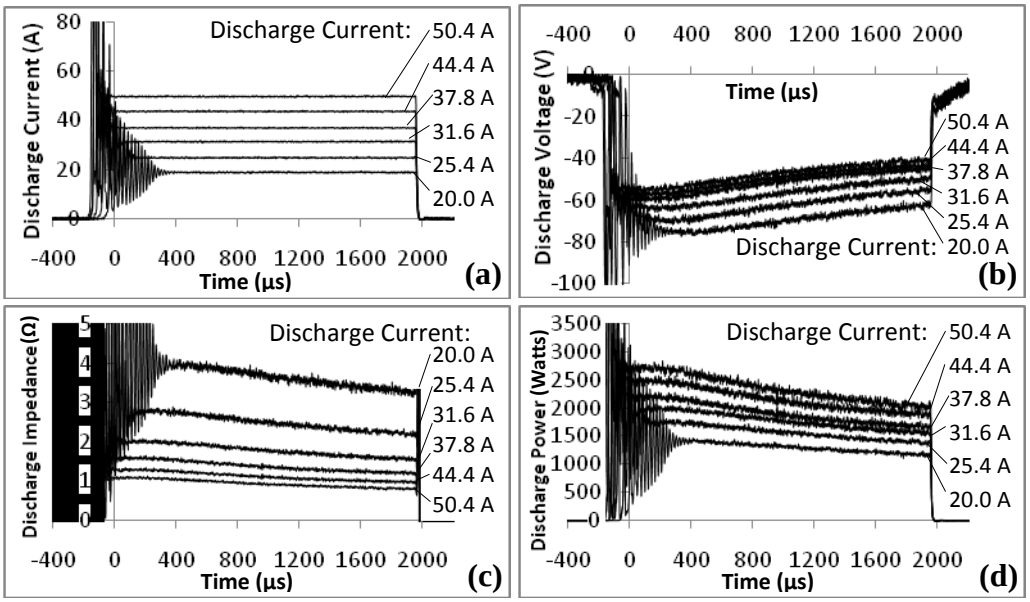

FIGURE 3. The source discharge current and voltage oscilloscope traces for different discharge currents. The discharge impedance and power are calculated from the current and voltage.

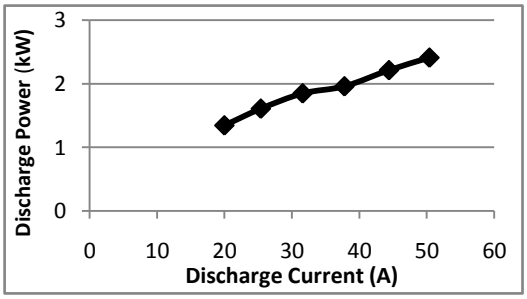

FIGURE 4. The variation of discharge power with discharge current.

The extraction voltage power supply is voltage regulated and is kept constant at 18.6 kV for all the experiments presented in this paper. The beam energy is also kept at 65 keV and the solenoid settings are left unchanged at 0.19 T, 0.17 T and 0.30 T. Figure 5 shows how the extraction current increases as the discharge current is increased.

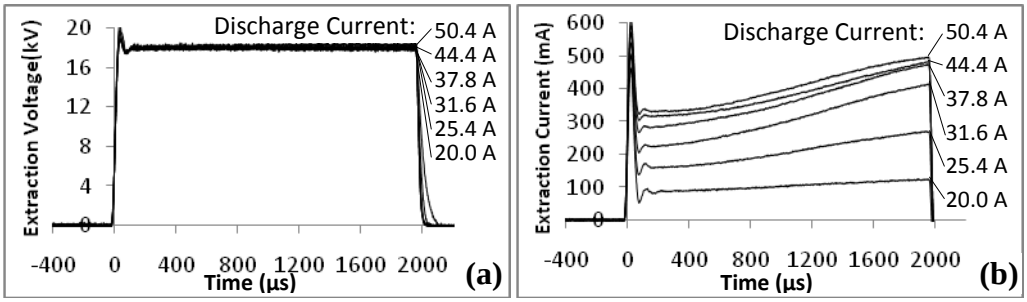

FIGURE 5: Extraction voltage pulse and current for different discharge currents.

Figure 6 shows the beam current measured at T1 for different discharge currents for a 2 ms long beam pulse. As the discharge current is reduced below 50 A the average beam current decreases but the droop decreases also, and for currents below 25 A the beam current is almost flat. The noise on the front of the H^- beam current is caused by noise at the start of the discharge becoming more severe and creeping into the extraction region. The noise present throughout the pulse is pickup from the high-frequency switching of the LEBT solenoid power supplies, and is not a real feature of the beam current.

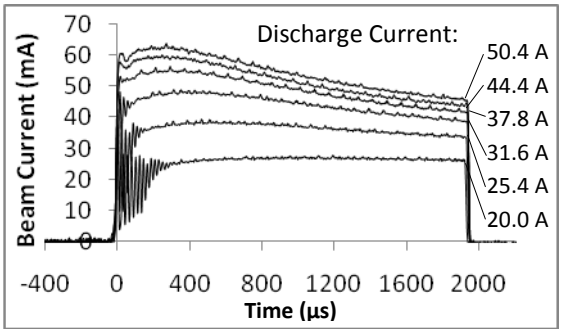

FIGURE 6. Variation in H^- beam current pulse shape for different discharge currents for 2 ms pulse lengths.

Figure 7 shows how the H^- beam current as measured by each of the toroids increases as the discharge current increases. For higher discharge currents the rate of increase of beam current becomes slower.

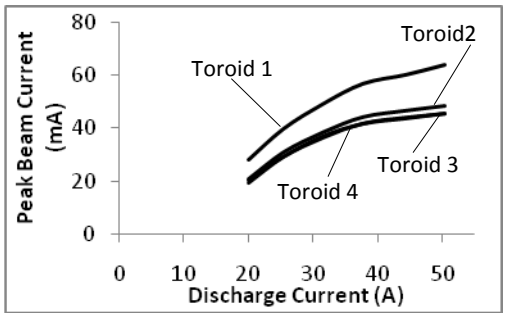

FIGURE 7. Variation in peak beam current measured at each of the 4 toroids for different discharge currents for 2 ms pulse length.

Vary Discharge Repetition Rate

The effect on the H^- beam current of reducing the discharge repetition rate is shown in figure 8. As the repetition rate is reduced the beam current increases and the droop decreases. For a 50 Hz discharge the beam current starts at 50 mA but droops to 30 mA at 2 ms. The shape of the beam current changes as the repetition rate is reduced; for lower repetition rates the beam current first rises then droops. At each repetition rate, source cooling is modified to keep the electrode temperatures approximately constant and the source is given time to stabilise.

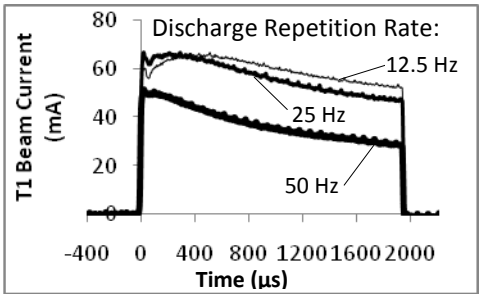

FIGURE 8. Variation in beam current in T1 for different discharge repetition rates.

Vary Hydrogen Flow Rate

Hydrogen at a static pressure of 600 mBar is pulsed into the ion source via a piezoelectric valve. The timing is kept constant: a 200 µs long pulse, triggered 800 µs before the start of the discharge and 1000 µs before the start of the extraction voltage pulse. By varying the amplitude of the voltage applied to the piezoelectric valve, the valve can be made to open wider and the amount of hydrogen delivered to each discharge pulse varied. The average hydrogen flow rate is measured using a flow meter near the hydrogen bottle.

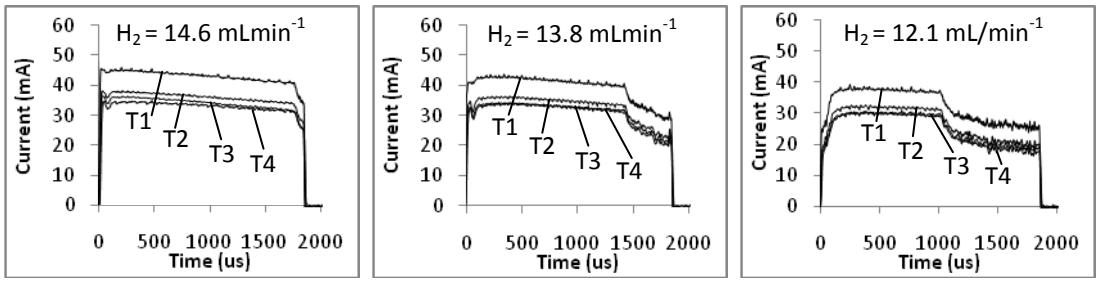

FIGURE 9. The variation in beam current for different hydrogen flow rates.

Figure 9 shows how the H^- beam current as measured by the toroids varies as the hydrogen flow rate is decreased. As the amount of hydrogen delivered to the discharge is reduced, the peak beam current starts to drop and a notch appears in the back of the pulse indicating hydrogen starvation. This phenomenon is only observed for discharges longer than 1000 µs. Increasing the hydrogen flow rate beyond 15 mLmin^{-1} does not further increase the beam current.

Emittance Scans

A pair of slit-slit emittance scanners in the diagnostics vessel after the LEBT are used to measure the horizontal and vertical emittances during the 2 ms beam pulse. Figure 10 shows emittance phase space plots at the beginning, middle and end of the 2 ms beam pulse for a 50 A 25 Hz discharge. The horizontal and vertical normalised r.m.s. emittances of approximately 0.3 πmm.mrad. Emittances are calculated using the SCUBEEx algorithm [2].

Figure 11 shows how the horizontal and vertical emittances, Twiss alphas and betas, vary along the 2 ms pulse for three different source conditions.

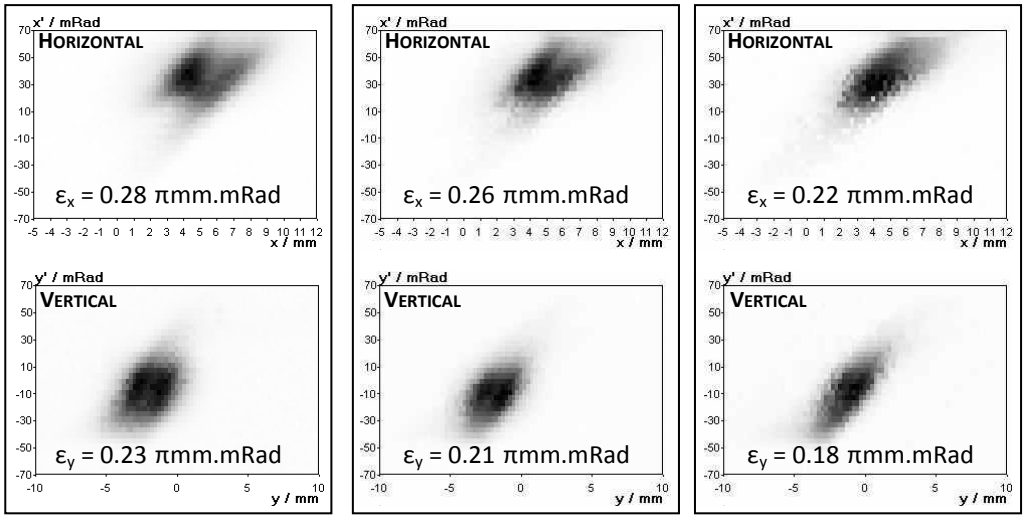

(a) Start: 210 μs (b) Middle: 1050 μs (c) End: 1943 μs

FIGURE 10. Phase space emittance plots at the start, middle and end of the 2 ms beam pulse for a 50 A 25 Hz discharge. All emittances are normalised r.m.s. The horizontal offset is caused by an alignment problem that has now been fixed.

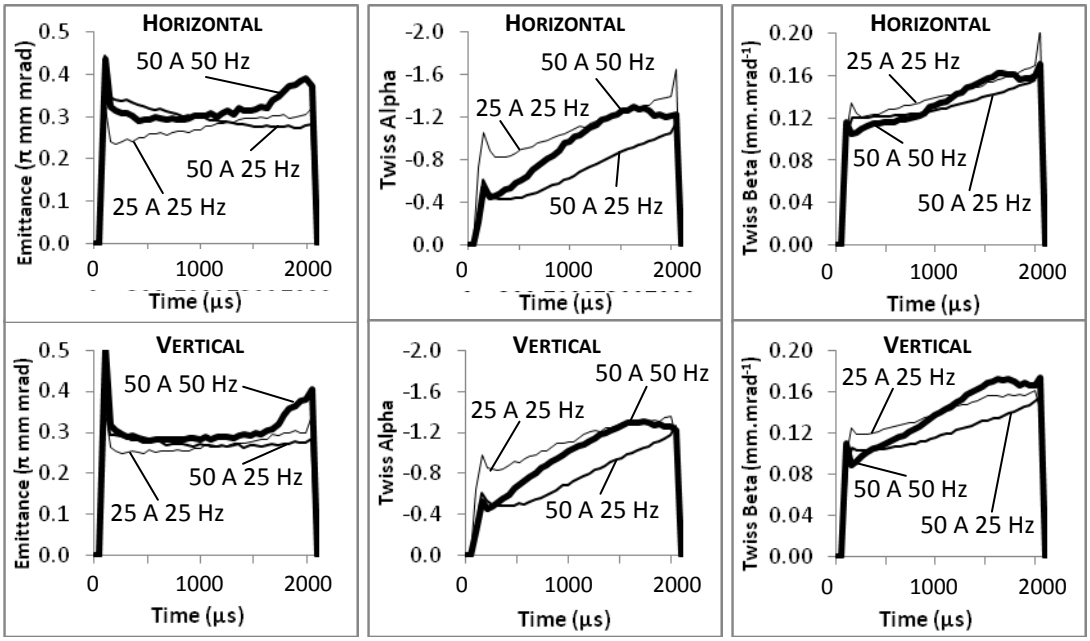

(a) Emittance (b) Twiss Alpha (c) Twiss Beta

FIGURE 11. Emittance and Twiss parameters versus time, for three different combinations of discharge current and discharge repetition rate.

DISCUSSION

Vary Discharge Current

The discharge current has a significant effect on both the magnitude and shape of H^- beam current produced as shown in figure 6. For higher discharge currents the beam current droop becomes significant. There are two main factors that could cause this droop:

Increased plasma density

Higher discharge currents produce an increased plasma density, which leads to more Cs being desorbed from the cathode surfaces by increased bombardment of H^+ and Cs^+. This pushes the level of Cs coverage away from its optimum for H^- production. Also H^- that are produced at the cathode surface are more likely to be stripped of their extra electron as they pass through the increased plasma density on their way to the extraction region.

Greater surface temperature change during the discharge

Figure 12 shows how the cathode surface temperature rises during the discharge then falls after the discharge is over. (See figure 4 for actual measured discharge powers.) The cathode surface temperature shown is calculated using transient 3-dimensional finite element analysis [3]. As the power in the discharge increases, the cooling is increased to maintain the same steady state temperature, but the transient surface temperature change increases. For higher discharge currents this change can be as high as 100°C for a 2 ms long discharge; this could be enough to push the level of Cs coverage away from the optimum for H^- production.

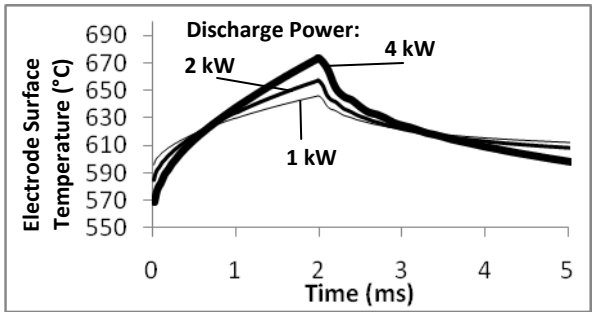

FIGURE 12. Transient 3D finite element modelling calculations of rise in cathode surface temperature during the discharge for different discharge powers.

Increasing the discharge current also leads to an increase in the rate at which the extraction current rises during the pulse (see figure 5). As the H^- beam current does not increase during the pulse this implies that more electrons are extracted near the end of the pulse which suggests that the electron density in the plasma also increases near the end of the discharge. This could possibly be caused by the depletion of surface caesium and hence the extracted H^-/e^- ratio goes down.

Vary Discharge Repetition Rate

The amount of droop in the beam current can also be altered by changing the discharge repetition rate as shown in figure 8. Leaving longer between pulses reduces the beam current droop. Cs vapour is continuously fed into the source, so leaving longer between pulses gives more time for Cs to build up on the electrode surfaces before the discharge comes on again.

Vary Caesium Oven Temperature

Figure 13 shows how the Cs vapour pressure varies with temperature [4]. Increasing the Cs oven temperature from 160°C to 190°C should produce a fourfold increase in vapour pressure. However initial experiments have failed to show an improvement in the amount of droop when the Cs oven temperature is varied in this range.

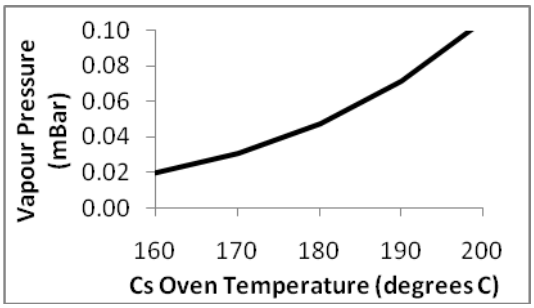

FIGURE 13. Cs vapour pressure versus temperature.

Vary Hydrogen Flow Rate

For a typical flow rate of 15 ml/minute of H_2 into the source at a static pressure of 0.6 Bar above atmosphere at a temperature of 15°C this gives a flow rate of:

$$\frac{\left(\frac{15\times10^{-3}}{60\times50}\right)\times1.6\times\left(\frac{273}{273+15}\right)\times2}{22.414} = 4\times10^{17}\text{protons per pulse}$$

For a 50 A 2.2 ms discharge, the total number of charge carriers in the discharge is:

$$50\times2.2\times10^{-3}\times1.602\times10^{-19} = 7\times10^{17}\text{charge carriers per pulse}$$

The charge carriers in the discharge are predominantly electrons and protons, with a small contribution from caesium and molybdenum ions and other ion species. The similarity between the number of protons delivered to the discharge and the number of charge carriers in the discharge is striking. The notch in the back of the H^- beam current pulse shown in figure 9 is most likely caused by a lack of protons available for the discharge or H^- production mechanism in the source.

Emittance Scans

Figure 11 shows how the beam emittance varies slightly along the length of the discharge. Phase rotation during the beam pulse can be seen in figure 10 which can be confirmed by the decreasing value of Twiss alpha in figure 11.

Space charge neutralisation of the beam occurs in the first 100 μs or so of the beam. For long beam pulse lengths phase rotation and a slight increase in emittance can be explained by loss of compensating particles. The neutralised beam no longer traps the compensating particles and they drift out of the beam, causing the beam to slowly blow up.

Figure 14 shows the beam brightness: $\frac{I_b}{8\pi\epsilon_x\varepsilon_y}$ for 3 different source conditions. When the source is running at 50 Hz with a 50 A discharge there is a significant drop in source brightness along the 2 ms beam pulse. Halving the repetition rate allows for an almost constant brightness throughout the pulse. Reducing the current to 25 A at 25 Hz yields a similar drop in brightness which implies that at 25 A the plasma density in the discharge is not high enough to sustain a high brightness beam.

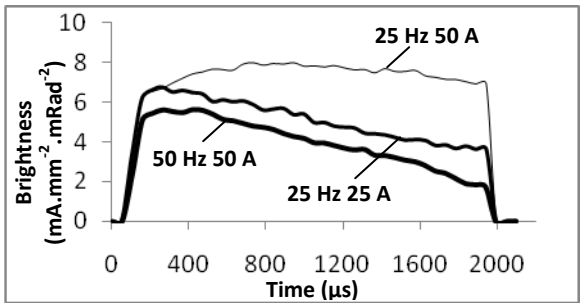

FIGURE 14. Variation in beam brightness for different discharge rep. rates and currents.

CONCLUSIONS

The physics of the operation of the source is complex and dynamic and requires further work to fully explain all the results presented in this paper. To produce a 50 Hz, 2 ms flat beam pulse it is clear that something must be done to keep the electrode surfaces in the optimum condition for H^- production. Increasing Cs flux does not seem to reduce the beam current droop. A possible way forwards is to increase the electrode surface area. Increasing the electrode surface area reduces the surface power density and reduces the transient temperature rise. It will also reduce the bombardment flux that causes Cs desorption from the electrodes surfaces. This has been successfully demonstrated by Smith and Sherman [5] with a x4 scaled source.

REFERENCES

1. D.C. Faircloth S. Lawrie, A. P. Letchford, C. Gabor, P. Wise, M. Whitehead, T. Wood, M. Westall, D. Findlay, M. Perkins, P. J. Savage, D. A. Lee, J. K. Pozimski, Review of Scientific Instruments, Volume 81, Issue 2, (2010).
2. Stockli M. P. et al., AIP Conf. Proc. 639, 135 (2002).

3. D.C. Faircloth, J. W. G. Thomason, M. O. Whitehead, W. Lau and S. Yang, Review of Scientific Instruments, Volume 75, Number 5, (2004).
4. J. B. Taylor, I. Langmuir, Phys. Rev. 51, 753 (1937)
5. H. V. Smith and J. Sherman, "H– and D– scaling laws for Penning Surface-Plasma Sources", Review of Scientific Instruments, Vol 65 (1), pp. 123-128 (1994).